EuPA Open Proteomics 10 (2016) 42–49

Contents lists available at ScienceDirect

EuPA Open Proteomics

journal homepage: www.elsevier.com/locate/euprot

Comparative proteomic analysis of malignant pleural mesothelioma: Focusing on the biphasic subtype

Laura Giusti[a], Federica Ciregia[a], Alessandra Bonotti[b], Ylenia Da Valle[a], Elena Donadio[a], Claudia Boldrini[a], Rudy Foddis[c], Gino Giannaccini[a], Maria R. Mazzoni[a], Pier Aldo Canessa[d], Alfonso Cristaudo[c], Antonio Lucacchini[a,*]

[a] Department of Pharmacy, University of Pisa, Pisa, Italy
[b] Preventive and Occupational Medicine, University Hospital of Pisa, Pisa, Italy
[c] Department of Translational Research and of New Technologies in Medicine and Surgery, University of Pisa, Pisa, Italy
[d] Dipartimento Ospedaliero Medico 2 dell' ASL5 Spezzino, La Spezia, Italy

ARTICLE INFO

Article history:
Received 18 November 2015
Received in revised form 11 January 2016
Accepted 13 January 2016
Available online 16 January 2016

Keywords:
Mesothelioma
Biphasic
Epithelioid
Proteomics
Serum amyloid
Nrf2

ABSTRACT

Malignant pleural mesothelioma (MPM) is a rare cancer originated from pleural mesothelial cells. MPM has been associated with long-term exposure to asbestos. In this work we performed a comparative proteomic analysis of biphasic pleural mesothelioma (B-PM).

Tissue biopsies were obtained from 61 patients who were subjected to a diagnostic thoracoscopy. 2D/MS based approach was used for proteomic analysis. The 22 proteins found differentially expressed in B-PM, with respect to benign, were analyzed by Ingenuity Pathways Analysis and compared with those obtained for epithelioid pleural mesothelioma (E-PM). A different activation of transcription factors, proteins and cytokines were observed between two subtypes.

1. Introduction

Malignant pleural mesothelioma (MPM) is an asbestos-induced, aggressive tumour, showing resistance to chemo- and radio-therapy and very poor outcome [1,2]. From a cytomorphologic point of view MPM can be distinguished in three different categories including epithelioid, biphasic and sarcomatoid. Biphasic tumours are characterized by the concomitant presence of epithelioid and sarcomatoid cells in close proximity or, more frequently, within distinctly separate areas of a tumour [3]. The response of biphasic tumour to treatment depends on the ratio of these two cellular subtypes. A tumour with the prevalence of sarcomatoid cells is associated with worse prognosis. Although a lot of efforts have been underway, aiming to identify the potential targets for novel therapies, no progress has been made in prolonging the median survival of 1 year from the time of diagnosis [4–6]. MPM is highly resistant to therapy, therefore surgery associated with treatments as radiotherapy and chemotherapy are preferred [7]. So, it is urgent to advance in our knowledge about the disease pathogenesis and to develop more effective therapies for different subtype of mesothelioma. Our group has recently performed a comparative proteome analysis between epithelioid mesothelioma (E-PM) and hyperplasia tissue biopsies. We showed that E-PM samples evidenced an altered expression of nuclear lamin and filament related proteins, in addition to confirming the validity of calretinin as a potential biomarker in the differential diagnosis of MPM [8]. In the present study we extended the comparative proteomic analysis to the biphasic mesothelioma (B-PM) searching for proteins that may play a role in the transition from epithelioid to the most aggressive biphasic phenotype.

2. Materials and methods

2.1. Materials

IPG strips pH 3–10 NL and dry strip cover fluid were purchased from GE Health Care Europe (Uppsala, Sweden). The ECL detection system was purchased from PerkinElmer (MA, USA). Anti-S100A11 (calgizzarin), anti-serum amyloid A1(SAA1) and anti-chloride intracellular channel protein 3 (CLIC3) specific primary antibodies

* Corresponding author at: Department of Pharmacy, University of Pisa, Via Bonanno, 6, 56126 Pisa.
E-mail address: antonio.lucacchini@farm.unipi.it (A. Lucacchini).

http://dx.doi.org/10.1016/j.euprot.2016.01.006

were from Abcam, (Cambridge, UK). Anti-γ enolase (ENO2), was from Cell Signaling Technology (MA, USA). Goat anti-rabbit IgG-HRP conjugate secondary antibody was from stress gene. All other reagents were acquired from standard commercial sources and were of the highest grade available.

2.2. Patients

Sixty-one patients were enrolled at the time of diagnosis before beginning any therapeutic treatment. Tissue biopsies were obtained from patients who were subjected to a diagnostic thoracoscopy. After histological examination, 23 samples were classified as E-PM, 10 samples as B-PM, 14 samples as benign (seven pleural inflammation and seven hyperplasia), and 14 samples as lung carcinoma (nine adenocarcinoma and five squamous cells carcinoma). Benign samples were used as negative control, while lung carcinoma samples were used in the validation step as positive control. Each sample was coded directly at the moment of collection, in order to avoid any personal identification. Table 1 shows the clinical characteristics of patients.

2.3. Ethics statements

The study methodologies were conformed to the standards set by the Declaration of Helsinki and were approved by the Local Ethics Committee and signed consent forms were obtained from all patients.

2.4. Protein preparation from biopsies

Proteins were precipitated from the phenol-ethanol supernatant obtained after treatment with TRIzol® reagent (Life technologies, UK), the resulting pellets were resuspended in rehydration solution (7 M Urea, 2 M thiourea, 4% CHAPS, 60 mM DTT, 0.002% bromophenol blue) and incubated for 30 min at room temperature. After incubation, the samples were centrifuged for 10 min at 14,000 × *g* to remove undissolved material. Protein concentrations were measured with a RC-DC protein assay from Bio-Rad, using bovine serum albumin as standard. All samples were stored at −80 °C until analysis.

2.5. 2D gel electrophoresis

According to histological analysis B-PM, E-PM and benign samples were used to constitute respectively three different pools for 2D analysis. IEF was carried out by using 18 cm Immobiline Dry-Strips (GE Healthcare) with a nonlinear, pH 3–10, gradient. Two-hundred micrograms of proteins were filled to 400 μL with rehydration buffer supplemented with 1.2% v/v IPG Buffer, pH 3–10 NL (GE Healthcare). IEF was performed at 16 °C on an Ettan IPGphor II apparatus (GE Healthcare) according to the previously described schedule [9]. After IEF, the strips were equilibrated as described, and SDS-PAGE was performed using the PROTEAN-II Multi Cell system (Bio-Rad) [10]. The gels were performed in triplicate.

2.6. Staining and image analysis

The gels were stained with Ruthenium II tris (bathophenanthroline disulfonate) tetrasodium salt (SunaTech Inc.) essentially as described by Aude-Garcia et al [11] with minor modifications [8,10].The acquisition on fluorescence of all gel images was performed by "ImageQuant LAS4010" (GE Healthcare). The images were analyzed with the SameSpots (version 4.1.3978., TotalLab, Ltd., UK) software as previously described [12]. The protein spots with a ≥2 fold of spot quantity change, $p < 0.05$ and q-value < 0.05 were selected and identified.

2.7. MS analysis and protein identification

Spots of interest were cut out from gel reference and the nano-LC-ESI-MS/MS analysis by LTQ-Orbitrap Velos was performed as previously described [10,12] Peak lists were generated from raw orbitrap data using the embedded software from the instrument vendor (extract_MSN.exe). The monoisotopic masses of the selected precursor ions were corrected using an inhouse written Perl script [13]. The peak list files were searched against the SwissProt/trEMBL database (Release 2013 03 of 06 March 2013) using Mascot (Matrix Sciences, London, UK). Human taxonomy (98 529 sequences) was specified for database searching. The parent ion tolerance was set at 10 ppm. Oxidation of methionine was specified in Mascot as a variable modification. Trypsin was selected as the enzyme, with one potential missed cleavage, and the normal cleavage mode was used. The mascot search was validated using Scaffold 4.4.5 (Proteome Software, Portland, OR). Only proteins matching with two different peptides with a minimum probability score of 95% were considered to be identified. The FDR at protein and peptide level was 0.0% and 0.2% respectively (Prophet). The reference limit to $p < 0.05$ for the probabilistic scores of MS/MS assignment was 45. When multiple proteins were identified in a single spot, the proteins with the highest number of peptides were considered as those corresponding to the spot.

2.8. Western blot analysis

For 1D western blot (WB), all samples were processed to validate different protein expressions found with 2D analysis. Aliquots (25 μg of proteins) of each sample (23 E-PM, 10 B-PM, 14 benign, and 14 lung carcinoma) were solubilized with a SDS sample buffer (Laemmli solution), and proteins were separated by 12% SDS-PAGE under reducing conditions and WB was carried out as previously described [14]. Before blocking the nitrocellulose, membranes were reversibly stained with 1 mM RuBP as previously described [10]. Specific primary antibodies were diluted in blocking buffer as follows: 1:2000 for anti-S100A11, anti-CLIC3, and anti-SSA1 and 1:500 anti-γ-enolase. The immunocomplexes were detected using a peroxidase labeled secondary antibody (goat anti-rabbit, 1:10000 dilution). Immunoblots were developed using the ECL detection system. The chemiluminescent images were acquired by LAS4010 (GE Healthcare). The experiments were performed in duplicate. Normalization was performed on total proteins loaded for each sample.

2.9. Statistical analysis

Statistical analysis of the three classes (B-PM, E-PM, and benign) of gels was performed by Same Spot (TotalLab, Ltd., UK). The software included the following statistical analysis calculations: Anova p-value, and false discovery rate (q-values). The OD of the proteins was expressed as a percentage of the volume (mean ± SEM). For the comparison of protein expression levels between different subtype of MPM and with respect to control samples (benign and carcinoma samples), the antigen-specific bands were quantified using the Image Quant-L (GE Healthcare). The significance of the differences (p-value ≤ 0.05) was calculated by the Mann–Whitney test.

2.10. Signaling pathway analysis

Proteins differentially expressed, were functionally analyzed through the use of QIAGEN's Ingenuity Pathway Analysis (IPA,

Table 1
Clinical data of all cases included in the study.

		MPM	BPM	Negative control	Positive control
Number		23	10	14	14
Gender (%)	Male	20 (87)	9 (90)	9 (64)	7 (50)
	Female	3 (13)	1 (10)	5 (36)	7 (50)
Age	Mean	62.8	66.5	63	67
	Range	35–80	47–83	55–82	57–81
Smoke (%)		5 (22)	2 (20)	2 (14)	6 (43)
Asbestos exposure (%)		16 (70)	6 (60)	5 (36)	7 (50)
Stage	I	NA	NA	NA	3 (21)
	II	18 (78)	3 (30)	NA	8 (57)
	III	5 (22)	7 (70)	NA	2 (14)
	IV	NA	NA	NA	1 (7)
Mesothelioma histology (%)	Epithelial	23 (100)	NA	NA	NA
	Biphasic	NA	10 (100)	NA	NA
Cancer histology (%)	Squamous cell carcinoma	NA	NA	NA	6 (43)
	Adenocarcinoma	NA	NA	NA	8 (57)
Benign histology (%)	Pleural inflammation	NA	NA	7 (50)	NA
	Hyperplasia	NA	NA	7 (50)	NA

NA: not applicable.

QIAGEN Redwood City, USA. www.qiagen.com/ingenuity) with the aim to determine the predominant canonical pathways and interaction network involved. Swiss-Prot accession numbers and official gene symbols were inserted into the software along with corresponding comparison ratios. Using the direction of change of the proteins in our data set, the downstream effects analysis was performed and the likely effect on disease and cell biological processes was evaluated. Moreover, a comparison of the analysis obtained by the proteomic profiles of B-PM and E-PM with respect to benign, was created and the upstream regulators whose activity appears to change in significantly manner according to the activation *z*-score value, were showed.

3. Results

3.1. Comparative proteomic analysis of MPM subtype biopsies

A differential analysis among B-PM, E-PM and benign was performed using 2DE followed by nano-LC-ESI-MS/MS. A representative image of B-PM samples is shown in Fig. 1A. After computational comparison of images obtained by different classes (B-PM, E-PM and benign), 26 protein spots were found to be differentially expressed with $\geq$2 fold change of mean value spot intensities in the B-PM with the respect to benign samples. These protein spots collapsed into the identification of 22 different

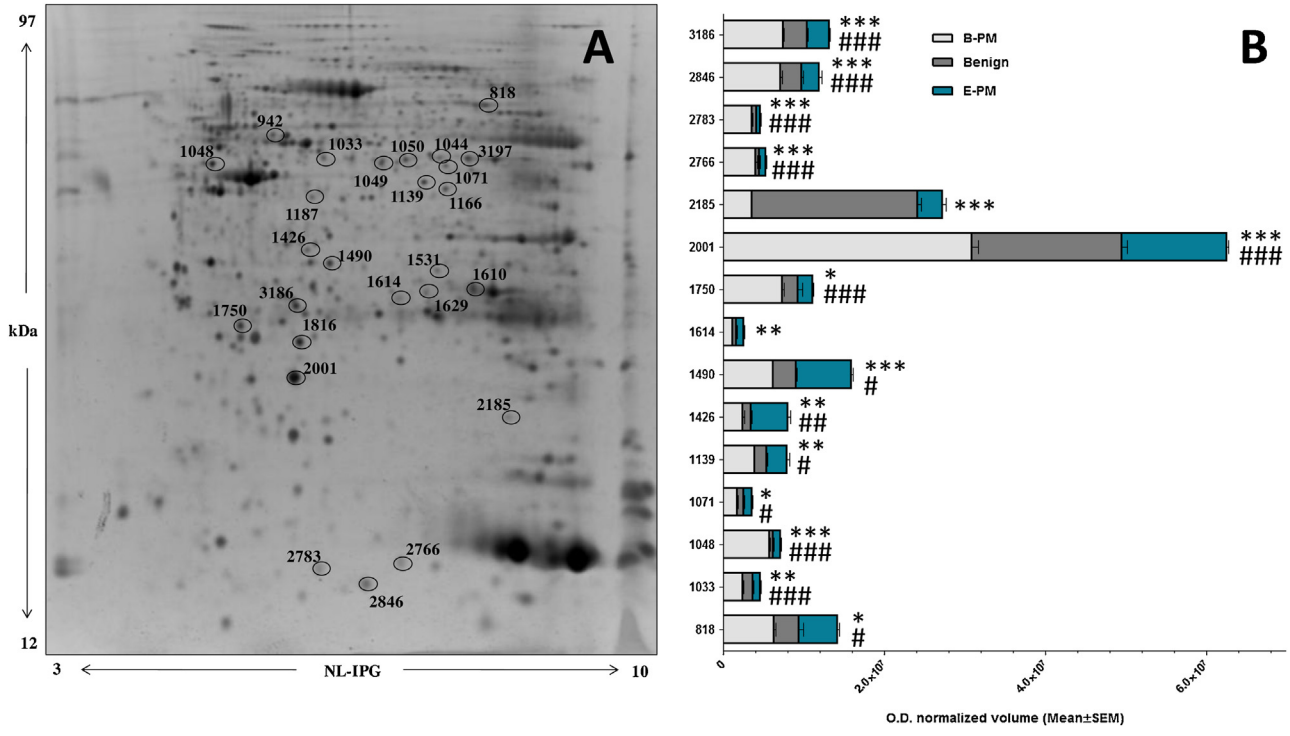

Fig. 1. (A) Representative 2D gel map of B-PM. Spots circled indicate all the proteins identified by nano-LC-ESI MS/MS and the spot numbers are reported in Table 1. (B) Histograms of the normalized OD density volumes (mean ±SEM) of the protein spots found in significantly different quantities from the comparisons. Significant differences are based on ANOVA; B-PM vs benign ($^{*}p < 0.05$, $^{**}p < 0.01$, $^{***}p < 0.001$); B-PM vs E-PM ($^{\#}p < 0.05$, $^{\#\#}p < 0.01$, $^{\#\#\#}p < 0.001$).

Table 2
MS/MS data of protein spots differentially expressed, together with statistical analysis.

#	ProteinName	ID	MW		pI		Match	Cov	Best Ion	BPM/benign		B-PM/E-PM		E-PM/benign	
			th	obs	th	obs	pep.	(%)	Score	FV	p-value	FV	p-value	FV	p-value
818	Alpha-enolase	P06733	47	53	7.0	6.8	6	20	82.2	2	0.0194	1.3	0.0162	1.6	ns
942	Keratin, type II cytoskeletal 7	P08729	51	49	5.4	5.3	13	34	80.8	3	0.0007	1.2	ns	3.7	0.0004
1033	Dolichyl-diphosphooligosaccharide--protein glycosyltransferase 48 kDa subunit	P39656	51	45	6.1	5.6	3	8	78.9	2	0.0038	2.6	0.0001	1.3	ns
1044	Alpha-enolase	P06733	47	44	7.0	6.3	12	39	102.6	2.1	0.0125	1.3	ns	1.5	ns
1048	Gamma-enolase	P09104	47	44	4.9	4.8	3	9	74.8	12.2	0.0007	6	0.00002	2	ns
1049	Rab GDP dissociation inhibitor beta	P50395	51	44	5.0	5.9	7	16	74.1	2.3	0.0074	2	0.0157	1.2	ns
1050	Rab GDP dissociation inhibitor beta	P50395	51	44	5.0	6.1	15	36	80.2	2	0.0050	1.4	ns	1.4	ns
1071	Alpha-centractin	P61163	43	43	6.2	6.3	7	28	121.9	2.2	0.0119	1.7	0.0180	1.3	ns
1139	Septin-2	Q15019	41	41	6.1	6.2	6	30	103.9	2.6	0.0013	1.5	0.0373	1.7	ns
1166	Actin-related protein 2	P61160	45	41	6.3	6.3	4	14	71.4	2.7	0.0060	2.1	0.0077	1.3	ns
1187	Fibrinogen beta chain	P02675	56	40	8.5	5.5	6	19	109	4.4	0.0003	2.5	0.0021	1.8	0.0001
1426	Annexin A8-like protein 2	Q5VT79	37	34	5.4	5.5	11	45	116.1	2.3	0.0010	1.9	0.0062	4.3	0.0001
1490	Annexin A4	P09525	36	33	5.8	5.6	6	19	91.3	2.2	0.0001	1.1	0.0177	2.4	0.0001
1531	Proteasome subunit alpha type-1	P25786	30	32	6.1	6.2	4	24	60.7	2	0.0450	1.2	ns	1.7	ns
1610	Carbonic anhydrase 1	P00915	29	30	6.6	6.6	8	43	99.9	1.8	0.0011	3.2	0.0015	1.7	0.028
1614	Chloride intracellular channel protein 3	O95833	27	30	5.9	6.0	3	20	72	2.4	0.0069	1.3	ns	1.9	ns
1629	Carbonic anhydrase 1	P00915	29	29	6.6	6.2	3	12	71.4	2.3	0.0049	3.2	0.0001	1.4	ns
1750	Apolipoprotein A-I	P02647	31	27	5.6	5.1	2	8	74.6	3.7	0.0229	3.9	0.0001	1.1	ns
1816	Glutathione S-transferase P	P09211	23	26	5.4	5.5	5	34	147.6	2.1	0.0002	1	ns	2.0	0.0002
2001	Peroxiredoxin-2	P32119	22	23	5.7	5.5	7	30	99.5	1.7	0.0004	2.4	0.00001	1.4	0.001
2185	Alpha-crystallin B chain	P02511	20	21	6.7	6.9	4	35	65.2	5.9	3,6E-07	1.1	ns	6.7	0.0003
2766	Serum amyloid A-1 protein	P0DJI8	14	14	6.3	6.0	3	38	83.0	9	0.0002	5	0.0008	1.8	ns
2783	Peroxiredoxin-1	Q06830	22	14	8.3	5.6	2	11	45	5.7	0.00001	7.1	0.0001	1.2	ns
2846	Protein S100-A11	P31949	12	12	6.6	5.9	4	31	59.2	2.7	0.0005	3.2	0.0023	1.2	ns
3186	Serum amyloid P-component	P02743	25	29	6.1	5.5	5	26	105.8	2.5	0.0002	2.7	0.00003	1.1	ns
3197	Alpha-enolase	P06733	47	44	7.0	6.6	15	44	112.2	2.2	0.0190	1.7	0.0358	1.3	ns

The highlighted proteins concur at a net separation between BPM and other classes, after PCA analysis.
FV, fold variation; ns, not significant.

proteins. Table 2 shows a list of identified proteins, molecular weight (MW), pI, score, and coverage values of MS/MS, the fold change in protein expression and their relative *p* values obtained from the selected comparisons (B-PM vs benign and vs E-PM). Rab GDP dissociation inhibitor β, α-enolase (ENO1) and carbonic anydrase I were present with more spots with different observed MW and/or pI suggesting the existence of protein isoforms or post-translational modifications. PCA analysis was performed by SameSpot (data not shown) and the proteins which concur at a net separation between BPM and other classes, are highlighted in Table 2. Fig. 1B shows the histogram of the proteins found differentially expressed in B-PM with respect to other classes.

3.2. Validation of B-PM proteins by WB analysis

According to PCA analysis, among proteins that resulted discriminating for MPM subtypes, we selected SAA1, S100A11, γ-enolase and CLIC-3. The validation of the different protein expression, obtained by immunoblot analysis, confirmed the different expression of all five proteins in B-PM with respect to the cognate E-PM subtype. Representative western blot are shown in Fig. 2. For each tested protein the OD of specific immunoreactive band was determined and the resulting mean values ± SEM were compared (B-PM vs benign, B-PM vs E-PM, BPM vs carcinoma). As shown in Fig. 2, it is confirmed significant the increase of expression only for SAA1 (p-value = 0.033) and γ-enolase (p-value = 0.042) in B-PM with respect to E-PM. A significant difference was also observed with respect the positive and negative controls ($p < 0.05$) for all four proteins.

3.3. IPA analysis

All the proteins derived from the proteomic comparison of B-PM vs benign were included in bioinformatic analysis to identify molecular and cellular functions and to investigate whether these proteins work together in specific networks. Moreover, all the proteins found up- and down-regulated may concur both in a downstream effects analysis and an upstream regulator analysis to predict if diseases/biological processes and transcription factors or genes could be activated or inactivated in agreement with *z*-score value (z-score > 2, and $p < 0.05$), respectively. Fig. 3A shows the downstream effects analysis. A significant decrease of activation state of synthesis of reactive oxygen species, respiratory system tumor and cell death with *z*-scores of −2.6, −2.2 and −2.2 respectively, was predicted. At the same time a significant increase (p = 0.0023) of activation of phagocytes was observed with z-score = 2. Finally, the canonical pathways coupled to downstream effects were showed. In addition, Fig. 3B shows the heat map generated by the comparison of IPA analysis (B-PM vs benign and E-PM vs benign) and displays the molecules predicted activated (red) or inactivated (green) in the two different MPM subtypes.

4. Discussion

MPM is a lethal asbestos-associate cancer with poor responsiveness to current chemotherapeutic drugs, which is often correlate to its high resistance to apoptosis [7,15]. This is particularly true for the biphasic, an aggressive MPM subtype. In

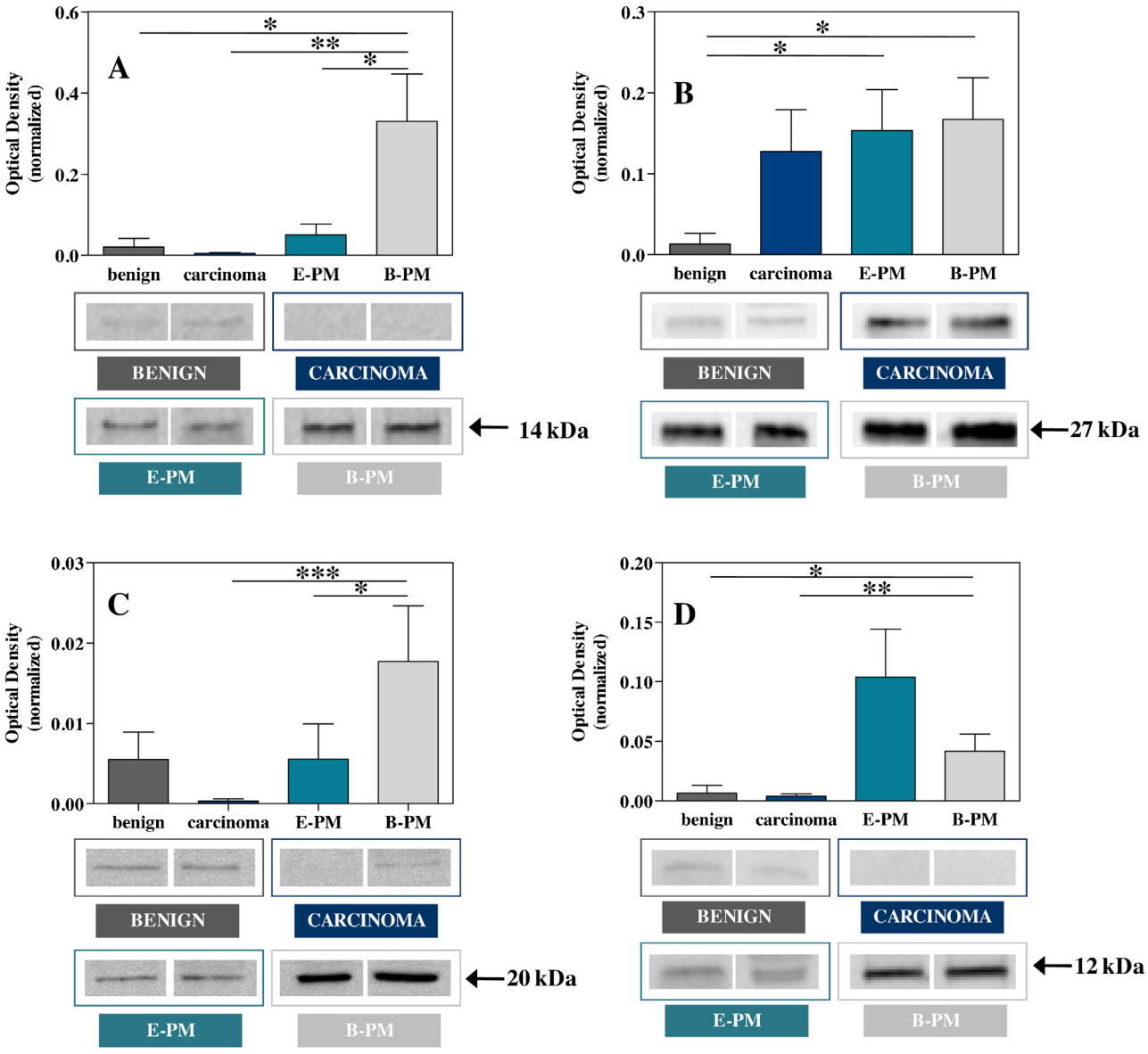

Fig. 2. Validation of SAA1 (A), CLIC3 (B), ENO2 (C), S100-A11 (D) by WB. The bar graph shows the mean ± SEM of the normalized OD values. The staining by rutenium was used as a protein-loading control. Statistical significance of the differences was calculated by Mann–Whitney ($^{*}p < 0.05$, $^{**}p < 0.01$ $^{***}p < 0.001$).

our previous report, using a combination of 2D and nano-LC-ESI/MS/MS spectrometry techniques, we performed a comparative analysis of proteomes of E-PM and benign biopsies' proteic extracts evidencing an altered expression of nuclear lamin and filament-related proteins [8]. In this work we extended the comparative proteomic analysis to the B-PM characterized by a combination of elements of epitheliod and sarcomatoid subtypes. Comparative analysis of each MPM subtype with benign defined a panel of 22 proteins that showed significant values of increase in B-PM but not in E-PM, exception for Keratin type II cytoskeletal 7 (KRT7), Annexin A8-like protein 2 (ANXAA8L2), Annexin A4 (ANXAA4), Carbonic anydrase I (CA1), Glutatione S-transferase P (GSTP1), Peroxiredoxin 2 (PRDX2) and Alpha-crystallin B chain (CRYAB), suggesting a peculiar biphasic protein profile. Moreover, 13 proteins showed to discriminate B-PM with high fold changes. By western blot analysis, the differences of expression were confirmed for 4 proteins (γ-enolase, SAA1, protein S100A11, CLIC3) but the capability to differentiate B-PM from E-PM was confirmed for γ-enolase and SAA1, not for S100A11 and CLIC3.

In vertebrate organisms three isoenzymes of enolase, expressed by different genes, are present: α-enolase (ENO1) is ubiquitous; β-enolase (ENO3) is muscle-specific and γ-enolase (ENO2) is neuron-specific [16]. In B-PM samples we found a significant increase of two isoforms of enolase, the ENO1 and the ENO2. The latter appears to give the higher difference of expression in B-PM when compared with benign samples, as confirmed also by western blot analysis. ENO2 has been suggested as a tumour marker and it is used in diagnosis and prognosis of cancer; however, the mechanisms enrolling it in malignant progression remain elusive [16,17]. ENO2 might therefore have a multifunctional role in cancer progression: as glycolytic enzyme it participates to accelerate the glycolysis, which supports increased tumour cells metabolic demands and enables their proliferation [18]. An additional role of ENO2 in cancer progression is its involvement in actin remodeling and consequently in promotion of migration and invasion of tumour cells [17]. Finally, noteworthy, the role of ENO2, suggested by Soh et al. [19] in breast epithelial cell and urothelial cell cancers, provides evidence that environmental

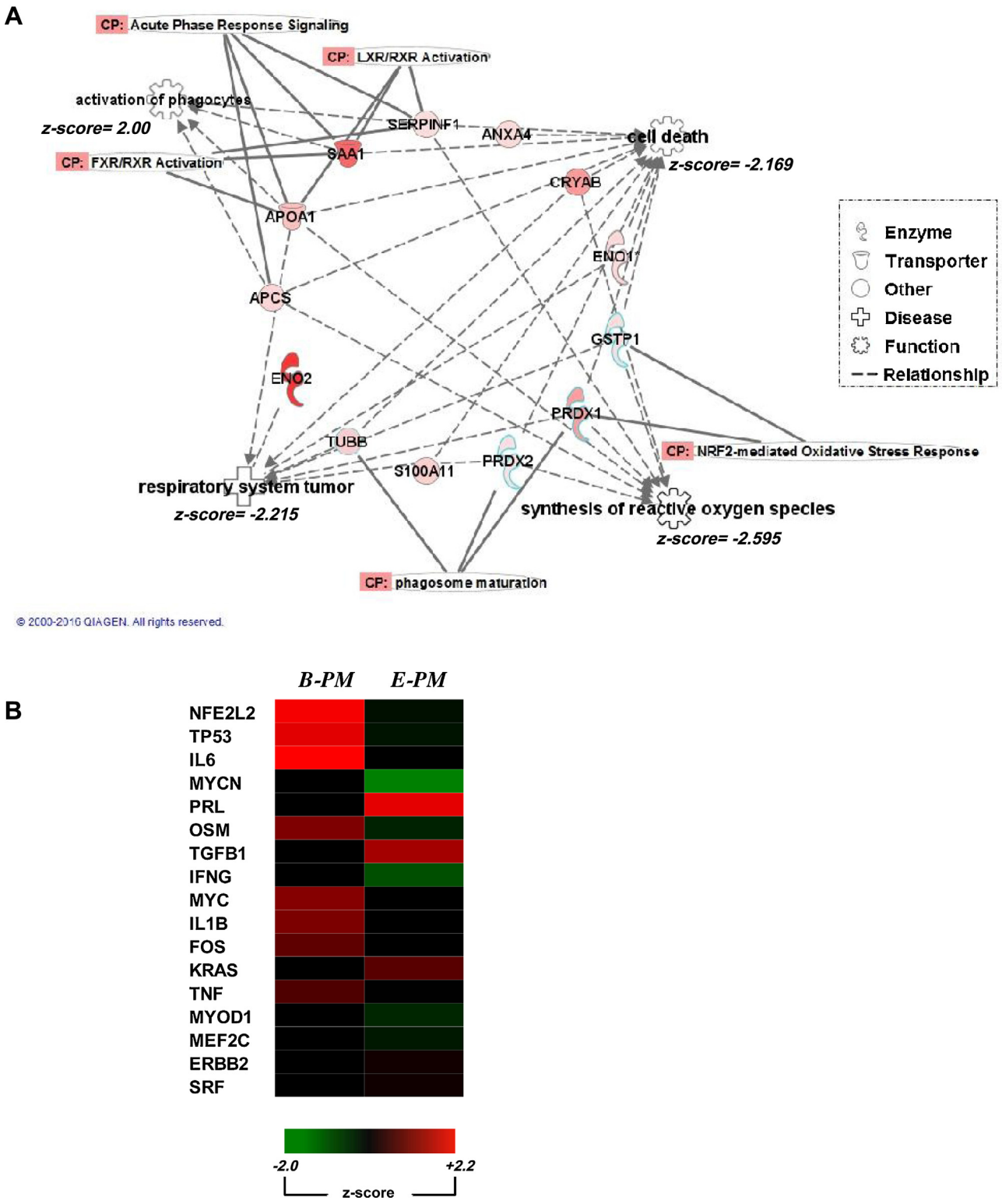

Fig. 3. (A) Analysis of downstream effects coupled to the most significantly affected canonical pathways and diseases/functions in BPM. (B) Heat map showing the activated (red) or inactivated (green) predicted molecules in two different conditions: B-PM and E-PM. The brighter the color, the more intense the change will be.

carcinogenic pollutants, such as cadmium and arsenic, might cause changes in epigenetic regulation of genes, which specifically affect the expression and function of ENO2. In our view, the expression of different isoforms of this enzyme could be correlated to different features of MPM subtypes. Indeed, we previously showed a reduction of ENO3 in E-PM [8] but not difference of expression of other two isoforms was observed.

A very intriguing matter is the peculiar and high increase observed for SAA1 and SAP belonged to the acute phase proteins, that are produced in response to infections and also to some non infectious insults [20]. In the contest of inflammation, SAA1 has been described to induce cytokines expression [21]. to modulate cell adhesion and migration [22] and to binding laminin [23]. In neoplastic diseases, SAA1 induces the increase of expression of

MMP2 and MMP9 leading to an excess of degrading activity that is supposed to be linked to the invasive character of tumour cells [24,25]. On the other hand, in the lung, SAA1 should not be considered alone as a specific biomarker of lung cancer since its increase is high also in the smokers [26]. SAP is a member of pentraxin family and presents a 66% of homology with C-reactive protein [27,28]. In humans, the levels of SAP in the plasma are relatively constant. In mice, SAP acts as an acute phase protein, with levels rising up following an inflammatory insult [29]. SAP also inhibits fibrosis, by inhibition of fibrocyte differentiation and regulating macrophage polarization [30]. Moreover, SAP induces the production of anti-inflammatory cytokines such as IL-10 and IL-6, inhibits pro-fibrotic M2a macrophages, and promotes the formation of immuno-regulatory Mreg macrophages [27]. In our context we could speculate that the increase of SAP might be a protective response to the injury induced by asbestos fibers.

Among the validated proteins, the increase of CLIC3 values was found in all types of cancer. CLIC3, together with CLIC4, was found to be overexpressed in MPM by Tasiopoulou et al. [31] who suggested that these proteins play a role in the transition from an epithelioid to a sarcomatoid phenotype. The trend to increase, that we highlighted in our samples, could be in agreement with this hypothesis.

Nonetheless, we believe that the difference in expression of the proteins found in B-PM subtype can help us to explore in deep the potential pathways and molecules (e.g. transcription factors) that could play a role in the differentiation of main features of two MPM hystotypes. Thus, we performed IPA analysis of 22 proteins found differentially expressed in B-PM with respect to benign samples and we compared it with that previously obtained for E-PM. Intriguingly, heat map shows a very different profile of activation. In fact, the nuclear factor erythroid 2-related factor 2 (NFE2L2 or Nrf2), the cytokine IL-6 and the tumour suppressor TP53 were significantly activated in B-PM, while were turned off in E-PM. On the other hand, prolactin (PRL) and N-myc proto-oncogene protein (MYCN) resulted activated and inhibited respectively, in E-PM. Nrf2 is a redox-sensitive transcription factor that controls the transcription of genes encoding various antioxidative and cyto-protective proteins [32]. Upon exposure to oxidants, Kelch-like ECH-associated protein (Keap1), a cytosolic repressor protein that binds to Nrf2, is inactivated. This event results in dissociation of Nrf2-Keap1 complex, with the consequent translocation of Nrf2 to the nucleus, where it induces the transcription and protein synthesis of detoxifying enzymes (as glutathione-S-transferase, GSTP1), antioxidant enzymes and proteins (as peroxiredoxin 1, PRDX1) [32]. In our IPA analysis the target molecules in dataset, which predicted the upstream Nrf2 activation, were SAP, SAA1, GSTP1, PRDX1 and proteasome subunit α-type 1 (PSMA1). The protective effect from oxidative insults, employed by products of Nrf2 activation, is responsible to attenuate efficacy of anticancer drugs by scavenging ROS, and enhance drug resistance. With respect to this point, and in agreement with our evidences, Lee et al. [33] demonstrated the importance of Nrf2 in cytoprotection, survival, and drug resistance on MSTO-211H, a biphasic cell line, suggesting the targeting of Nrf2 as a promising strategy for overcoming resistance to chemotherapeutics in MPM. As far as the IL-6 concerned, its role as mediator of pivotal processes is emerging, such as proliferation and chemoresistance within the mesothelioma microenvironment [34]. Although elevated serum concentration of IL-6 has been implicated as a poor prognostic factor in some advanced carcinomas, not yet a role in MPM has been established. However, there are evidences associating IL-6 with established poor prognostic factors of MPM, including trombocytosis and elevated protein reactive C (CRP) [35]. Similarly, our results suggest an upstream activation of Il-6 predicted by elevated levels of proteins of acute response such as SAP and SAA1, in addition to ENO2 and apolipoprotein 1 (APO1).

In conclusion, among all solid cancers, MPM is surely considered as one of the worse diseases in terms of its inherent chemoresistance, resulting in poor survival rates and disappointing responses to novel agents which have showed a promising activity in other tumours. In light of these facts, there is an obvious need to look for new therapeutic targets, together with the research of molecules, upstream regulators, and pathways involved in the different grade of malignancies and aggressiveness. Overall, our results confirm similarity and suggest divergence between two MPM subtypes. Their origin could be a different response of cells to the same detrimental agent (asbestos), which is achieved with a different activation or inhibition of transcription factors, obtaining different grade of malignancies.

Conflict of interest

The authors declare that they have no conflict of interest.

Acknowledgements

This research was supported by grant from the Ministero della Salute (to AC and AL) and from University of Pisa (Fondi per la Ricerca to AL).

References

[1] B.W. Robinson, R.A. Lake, Advances in malignant mesothelioma, N. Engl. J. Med. 353 (2005) 591–603.
[2] R. Ismail-Khan, L.A. Robinson, C.C. Williams Jr., C.R. Garrett, G. Bepler, G.R. Simon, Malignant pleural mesothelioma: a comprehensive review, Cancer Control 13 (2006) 255–263.
[3] D.W. Henderson, G. Reid, S.C. Kao, N. van Zandwijk, S. Klebe, Challenges and controversies in the diagnosis of malignant mesothelioma: part 2. Malignant mesothelioma subtypes, pleural synovial sarcoma, molecular and prognostic aspects of mesothelioma, BAP1, aquaporin-1 and microRNA, J. Clin. Pathol. 66 (2013) 854–861.
[4] C. Cao, D. Tian, C. Manganas, P. Matthews, T.D. Yan, Systematic review of trimodality therapy for patients with malignant pleural mesothelioma, Ann. Cardiothorac. Surg. 1 (2012) 428–437.
[5] J. Remon, N. Reguart, J. Corral, P. Lianes, Malignant pleural mesothelioma: new hope in the horizon with novel therapeutic strategies, Cancer Treat. Rev. 41 (2015) 27–34.
[6] A.R. Haas, D.H. Sterman, Malignant pleural mesothelioma: update on treatment options with a focus on novel therapies, Clin. Chest Med. 34 (2013) 99–111.
[7] W. Zhang, X. Wu, L. Wu, W. Zhang, X. Zhao, Advances in the diagnosis, treatment and prognosis of malignant pleural mesothelioma, Ann. Transl. Med. 3 (2015) 182.
[8] L. Giusti, Y. Da Valle, A. Bonotti, E. Donadio, F. Ciregia, T. Ventroni, R. Foddis, G. Giannaccini, G. Guglielmi, A. Cristaudo, A. Lucacchini, Comparative protomi analysis of malignant pleural mesothelioma evidences an altered expression of nuclear lamin and filament-related proteins, Proteomics Clin. Appl. 8 (2014) 258–268.
[9] L. Giusti, C. Baldini, L. Bazzichi, F. Ciregia, I. Tonazzini, G. Mascia, G. Giannaccini, S. Bombardieri, A. Lucacchini, Proteome analysis of whole saliva: a new tool for rheumatic diseases—the example of Sjögren's syndrome, Proteomics 7 (2007) 1634–1643.
[10] L. Giusti, V. Mantua, Y. Da Valle, F. Ciregia, T. Ventroni, G. Orsolini, E. Donadio, G. Giannaccini, M. Mauri, G.B. Cassano, A. Lucacchini, Search for peripheral biomarkers in patients affected by acutely psychotic bipolar disorder: a proteomic approach, Mol. Biosyst. 10 (2014) 1246–1254.
[11] C. Aude-Garcia, V. Collin-Faure, S. Luche, T. Rabilloud, Improvements and simplifications in in-gel fluorescent detection of proteins using ruthenium II tris-(bathophenanthroline disulfonate): the poor man's fluorescent detection method, Proteomics 11 (2011) 324–328.
[12] L. Giusti, P. Iacconi, Y. Da Valle, F. Ciregia, T. Ventroni, E. Donadio, G. Giannaccini, M. Chiarugi, L. Torregrossa, A. Proietti, F. Basolo, A. Lucacchini, A protomic profile of washing fluid from the colorectal tract to search for potential biomarkers of colon cancer, Mol. Biosyst. 8 (2012) 1088–1099.
[13] A. Scherl, Y.S. Tsai, S.A. Shaffer, D.R. Goodlett, Increasing information from shotgun proteomic data by accounting for misassigned precursor ion masses, Proteomics 8 (2008) 2791–2797.
[14] F. Ciregia, L. Giusti, A. Molinaro, F. Niccolai, P. Agretti, T. Rago, G. Di Coscio, P. Vitti, F. Basolo, P. Iacconi, M. Tonacchera, A. Lucacchini, Presence in the pre-

surgical fine-needle aspiration of potential thyroid biomarkers previously identified in the post-surgical one, PLoS One 8 (2013) e72911.
[15] B. Davidson, Prognostic factors in malignant pleural mesothelioma, Hum. Pathol. 46 (2015) 789–804.
[16] M.A. Isgrò, P. Bottoni, R. Scatena, Neuron-specific enolase as a biomarker: biochemical and clinical aspects, Adv. Exp. Med. Biol. 867 (2015) 125–143.
[17] T. Vizin, J. Kos, Gamma-enolase: a well-known tumour marker, with a less-known role in cancer, Radiol. Oncol. 49 (2015) 217–226.
[18] J.W. Kim, C.V. Dang, Multifaceted roles of glycolytic enzymes, Trends Biochem. Sci. 30 (2005) 142–150.
[19] M. Soh, J.R. Dunlevy, S.H. Garrett, C. Allen, D.A. Sens, X.D. Zhou, M.A. Sens, S. Somji, Increased neuron specific enolase expression by urothelial cells exposed to or malignantly transformed by exposure to Cd^{+2} or As^{+3}, Toxicol. Lett. 212 (2012) 66–74.
[20] S. Urieli-Shoval, R.P. Linke, Y. Matzner, Expression and function of serum amyloid A, a major acute-phase protein, in normal and disease states, Curr. Opin. Hematol. 7 (2000) 64–69.
[21] R. He, H. Sang, R.D. Ye, Serum amyloid A induces IL-8 secretion through a G protein-coupled receptor, FPRL1/LXA4R, Blood 101 (2003) 1572–1581.
[22] L. Xu, R. Badolato, W.J. Murphy, D.L. Longo, M. Anver, S. Hale, J.J. Oppenheim, J. M. Wang, A novel biologic function of serum amyloid A. Induction of T lymphocyte migration and adhesion, J. Immunol. 155 (1995) 1184–1190.
[23] J.B. Ancsin, R. Kisilevsky, Characterization of high affinity binding between laminin and the acute-phase protein, serum amyloid A, J. Biol. Chem. 272 (1997) 406–413.
[24] C. Paret, Z. Schön, A. Szponar, G. Kovacs, Inflammatory protein serum amyloid A1 marks a subset of conventional renal cell carcinomas with fatal outcome, Eur. Urol. 57 (2010) 859–866.
[25] M. Björklund, E. Koivunen, Gelatinase-mediated migration and invasion of cancer cells, Biochim. Biophys. Acta. 1755 (2005) 37–69.
[26] A. Rostila, A. Puustinen, T. Toljamo, K. Vuopala, I. Lindström, T.A. Nyman, P. Oksa, T. Vehmas, S.L. Anttila, Peroxiredoxins and tropomyosins as plasma biomarkers for lung cancer and asbestos exposure, Lung Cancer. 77 (2012) 450–459.
[27] G. Vilahur, L. Badimon, Biological actions of pentraxins, Vasc. Pharmacol. 73 (2015) 38–44.
[28] D. Xi, T. Luo, H. Xiong, J. Liu, H. Lu, M. Li, Y. Hou, Z. Guo, SAP: structure, function, and its roles in immune-related diseases, Int. J. Cardiol. 187 (2015) 20–26.
[29] P.T. Le, M.T. Muller, R.F. Mortensen, Acute phase reactants of mice: I. Isolation of serum amyloid P-component (SAP) and its induction by a monokine, J. Immunol. 129 (1982) 665–672.
[30] A.P. Castaño, S.L. Lin, T. Surowy, B.T. Nowlin, S.A. Turlapati, T. Patel, A. Singh, S. Li, M.L. Lupher Jr., J.S. Duffield, Serum amyloid P inhibits fibrosis through Fc gamma R-dependent monocyte-macrophage regulation in vivo, Sci. Transl. Med. 1 (2009) 5ra13.
[31] V. Tasiopoulou, D. Magouliotis, E.I. Solenov, G. Vavougios, P.-A. Molyvdas, K.I. Gorgoulianis, C. Hatzoglou, S.G. Zarogiannis, Transcrptional over-expression of chloride intracellular channels 3 and 4 malignant pleural mesothelioma, Comput. Biol. Chem. 59 (2015) 111–116.
[32] S.L. Slocum, T.W. Kensler, Nrf2: control of sensitivity to carcinogens, Arch. Toxicol. 85 (2011) 273–284.
[33] Y.J. Lee, D.M. Lee, S.H. Lee, Nrf2 expression and apoptosis in quercetin-treated malignant mesothelioma cells, Mol. Cells 38 (2015) 416–425.
[34] S.N. Abdul Rahim, G.Y. Ho, J.I. Coward, The role of interleukin-6 in malignant mesothelioma, Transl. Lung Cancer Res. 4 (2015) 55–66.
[35] T. Nakano, A.P. Chahinian, M. Shinjo, A. Tonomura, M. Miyake, N. Togawa, K. Ninomiya, K. Higashino, Interleukin 6 and its relationship to clinical parameters in patients with malignant pleural mesothelioma, Br. J. Cancer 77 (1998) 907–912.